DE GRUYTER

Biologia **71**/3: 247—255, 2016
Section Cellular and Molecular Biology
DOI: 10.1515/biolog-2016-0043

In vitro evaluation of indole-3-carboxaldehyde on *Vibrio parahaemolyticus* biofilms

Murugan Rajalaxmi, Vivekanandham Amsa Devi & Shunmugiah Karutha Pandian*

Department of Biotechnology, Science Campus, Alagappa University, Karaikudi – 630 004, Tamil Nadu, India; e-mail: sk_pandian@rediffmail.com

Abstract: This study was aimed to explore antibiofilm agents from the hitherto underexplored Palk Bay seawater bacteria. The cell free culture supernatant of the isolate *Marinomonas* sp. showed profound antibiofilm activity against *Vibrio parahaemolyticus* ATCC 17802. The active principle responsible for antibiofilm activity was identified as indole-3-carboxaldehyde (ICA) after bioassay guided purification and gas chromatography-mass spectrometry analysis. Further, *in vitro* antibiofilm activity of ICA was confirmed through light microscopy, confocal imaging, scanning electron microscopy and biofilm disruption studies. In addition, ICA efficiently reduced the swarming motility of the pathogen and promoted the swimming ability. Furthermore, the control of biofilms and swarming efficiency by quorum sensing pathway of the pathogen was modulated by ICA, which was substantiated using real-time analysis for *opaR*, *cpsA*, and *lafA* genes. This study divulged the efficacy of ICA as an antibiofilm agent against *V. parahaemolyticus in vitro*.

Key words: indole-3-carboxaldehyde; *Marinomonas* sp.; *Vibrio parahaemolyticus*; biofilm disruption; antibiofilm; seawater bacteria.

Abbreviations: BIC, biofilm inhibitory concentration; CFCS, cell-free culture supernatant; CLSM, confocal laser scanning microscopy; DPA, 2,6-di-O-palmitoyl-L-ascorbic acid; GC-MS, gas chromatography mass spectrometry; ICA, indole-3-carboxaldehyde; LB, Luria Bertani; LM, light microscopy; MIC, minimal inhibitory concentration; mLB, marine Luria Bertani; OD, optical density; QS, quorum sensing; SA, stearic acid; SEM, scanning electron microscopy; ZMB, Zobell marine broth.

Introduction

Marine infectious diseases cannot be under-appreciated as two third of the world's population depends on sea food. The marine host-pathogen-environment paradigm is inextricably linked, which opens the door for establishment, severity and outcome of these infectious diseases. Added to the fact, climatic change and antimicrobial resistance facilitate the proliferation of the diseases to a greater extent. Understanding the virulence mechanisms, by which the pathogen establishes the host interaction, is expected to result in the discovery of fruitful strategies to combat antimicrobial resistance. One such mechanism, which bacteria utilize to hide and protect themselves from antibiotics, is biofilm formation. Therefore, antivirulent agents, which prevent and disintegrate the biofilms, could be the drug of choice. It has been reported that the presence of clean surface in the marine ecosystem is due to the production of antifouling metabolites by existing microbial communities, either alone or in association with sessile marine macro-organisms, in order to prevent hazardous biofilms (Armstrong et al. 2000; Sayem et al. 2011). Hence, antibiofilm agents from such an ecosystem would render positive leads to manage the pathogenic biofilm trajectories.

Vibrio parahaemolyticus, a Gram negative pathogen, habituates marine and fresh water environment and infects the human population via ingestion of under cooked or raw seafood and also via the exposure of wounds in warm sea water, thereby causing vibriosis. Severity of the infection augments with gastroenteritis, septicemia and wound infection (Yeung & Boor 2004; Su & Liu 2007; Newton et al. 2012). Importance of the pathogenesis begins with epidemic and rare pandemic outbreaks (Ceccarelli et al. 2013; Chowdhury et al. 2013) and the causative strains were mostly found resistant to the already reported antibiotics (Sahilah et al. 2014; Shaw et al. 2014).

The pathogen initiates its life cycle in the host through biofilm formation, an exopolysaccharide matrix encasing the cells by providing essential nutrients for its growth and renders resistance to antibiotics than its planktonic counterpart. Further, in *V. parahaemolyticus*, biofilm mode of socialization is controlled by signaling cascade (also known as quorum sensing,

* Corresponding author

QS) via auto-inducers. In addition, the QS cascade regulates the swarming and swimming motility of the pathogen, virulence genes expression and consequently toxin production for disease development (Broberg et al. 2011). Hence the treatment strategy focusing on inhibiting the biofilm formation (via modulating the QS cascade) and disintegrating the pre-formed biofilms instead of arresting the cell growth could efficiently relegate the robustness of antimicrobial resistance.

Conventional antibiotics to date have mostly been obtained from soil microbial populations and synthetic library preparations. Overwhelmed with antibiotic resources, soil microbiota augments persistent infection with antimicrobial resistance. Hence, focus on marine microbiota would effectively render solution to the precarious scenario. Earlier studies have demonstrated the discovery of novel antibiofilm agents from marine microorganisms. The antibiofilm agents, such as 4-butylphenoic acid was explored from marine sediment bacterium *Bacillus pumilus* against various Gram-positive and Gram-negative bacteria (Nithya et al. 2011) and cyclo (L-leucyl-L-prolyl) from marine mangrove bacterium *B. amyloliquefaciens* against *Streptococcus mutans* (Gowrishankar et al. 2014). Furthermore, more than 200 natural marine compounds have been reported as prolific and promising eco-friendly antifoulants (Qian et al. 2015). Therefore, the current study was aimed at exploring seawater bacteria for antibiofilm agents against *V. parahaemolyticus*.

Material and methods

Bacterial strains and culture conditions

V. parahaemolyticus ATCC 17802 was taken as the target pathogen and maintained anaerobically at 30 °C with pH 7.5 ± 0.2 in marine Luria-Bertani (mLB) medium (3% NaCl in LB, Himedia Laboratories Pvt Ltd., India). For further experimental purposes, the pathogen was subcultured in mLB with 0.4 optical density (OD) at 600 nm (10^8 CFU/mL). Overall, 66 seawater bacterial isolates from Karankadu, Palk Bay, India, were screened for antibiofilm activity and all the isolates were maintained in Zobell marine broth (ZMB; Himedia Laboratories Pvt Ltd., India) at 28 °C. The positive isolate was identified as *Marinomonas* sp. through 16S rDNA sequencing (GenBank accession No. KC109734).

Bacterial extracts preparation and purification

One percent of *Marinomonas* sp. (v/v) was cultivated in ZMB at 28 °C for 48 h with 150 rpm in a shaking incubator. The culture was centrifuged to obtain the cell-free culture supernatant (CFCS) at 20,929× *g* for 10 min. The CFCS was then subjected to filtration using 0.2 mm membrane filter and equal volume of the filtrate was subjected to solvent extraction on polarity basis. Amongst the various solvents used, ethyl acetate extract exhibited better antibiofilm activity and the extract was evaporated and dried at room temperature. The dried form of the extract was weighed and re-dissolved in ethyl acetate and subjected for column chromatography at a flow rate of 1 mL/min using silica gel (60–120 mesh size, Merck, in 50 cm × 2 cm column). The solvents with increased polarity were used for fractionation. Further, the obtained individual fractions were dried and re-dissolved in methanol to accomplish a final concentration of 1 mg/mL, which was used for activity based screening. Finally, the separated active fraction was taken for gas chromatography mass spectrometry (GC-MS) analysis.

GC-MS analysis

The GC-MS analysis was performed in Shimadzu QP-2010 Ultra apparatus for the separated active fraction involving helium as the carrier gas, in a fused-silica capillary column (30 m × 0.25 mm length and 0.25 μm film thickness) with a flow rate of 1.21 mL/min. Injection of the sample was carried out in a split mode at the ratio of 1 : 10. The injector was maintained at 250 °C. Oven temperature of the column was set at 100 °C for 2 min. The set up was then programmed to 250 °C for 5 min. Finally, the temperature was increased to 280 °C for 25 min. Total run time was programmed for 40 min. The major constituents present in the separated bioactive fraction were analyzed using Wiley (http://www.sisweb.com/software/ms/wileysearch.htm) and NIST (http://www.sisweb.com/software/ms/nistsearch.htm) libraries.

Antibacterial activity and biofilm susceptibility assay

The major compounds identified through GC-MS analysis were tested for their biofilm and growth inhibitory potential against *V. parahaemolyticus* by static crystal violet assay and standard broth dilution assay as per the protocols described earlier (Salini et al. 2015). Indole-3-carboxaldehyde (ICA) (CAS: 487-89-8) procured from Sigma Aldrich, stearic acid (SA) (CAS: 57-11-4) from Alfa Aesar and 2,6-di-O-palmitoyl-L-ascorbic acid (DPA) (CAS: 4218-81-9) from TCI chemicals were used for the experiments. Assays were performed with mLB containing the bacterial suspension in test tubes (12 × 75 mm). The biofilm inhibitory concentration (BIC) and the minimal inhibitory concentration (MIC) were measured spectrophotometrically (SpectraMax M3, USA). Among the compounds screened, the active principle exhibiting antibiofilm activity alone was taken for further experiments.

In situ visualization and analysis of V. parahaemolyticus biofilm

The biofilm architecture of *V. parahaemolyticus* upon treatment with ICA was studied in a 24 well plate using 1 × 1 cm glass slides. The plate was incubated with 1% inoculum in 1 mL of mLB broth for 24 h at 30 °C. Biofilms were allowed to adhere to the glass slides, which were then stained and fixed as per the protocols described earlier (Gowrishankar et al. 2014). Absence and presence of the compound ICA (at its BIC) in mLB with *V. parahaemolyticus* were taken as the control and treated slides.

Light microscopy (LM)

The control and treated biofilm slides were examined with the magnification of × 400 in a Euromex light microscope (Model: GE3045, The Netherlands) and the images were acquired using the digital camera embedded system (Cmex camera, model: DC5000, The Netherlands).

Confocal laser scanning microscopy (CLSM)

The CLSM images of the control and treated biofilms on the glass slides (with the magnification of × 200) were acquired by Z stack analysis employed with Zen 2009 software (LSM 710, Carl Zeiss, Germany). Further, COMSTAT software was used to evaluate the different parameters of the images, i.e. maximum and average thickness, surface area and biovolume of the biofilms.

Table 1. List of genes used for the real time PCR study, with their role and nucleotide sequence of primers.

Gene	Role	Primer sequence (current study)	
		Forward	Reverse
opaR	Master QS regulator	TGTTGTCCGTCAGTTCTCGA	GTGCGGTTGGTAGACACAAA
cpsA	Capsule production	GGTTTTCTACGTCGCACCTC	CGACGCGCTTTTCCATCTTA
lafA	Lateral flagella production	GGGCGCAGTTACTTTCCAAA	AGACGGTTTGAGTTTGCACC
16S*rDNA*	Housekeeping gene	ACTCCTACGGGAGGCAGCAG	ATTACCGCGGCTGCTGG

Scanning electron microcopy (SEM)
In SEM analysis, samples were treated to critical point for drying and afterward coated with gold sputter. The images (with the magnification of × 5,000) were acquired using Hitachi S-3000H (Japan).

Effect of ICA on V. parahemolyticus pellicle
To arrive at the pre-formed biofilm collapsing concentration of ICA, *V. parahaemolyticus* biofilms were enabled to develop at the air liquid interface for 24 h in the test tubes (15 × 150 mm) containing 2 mL of mLB with 1% inoculum. Subsequently, the biofilms (pellicle) containing assay tubes were subjected to different concentrations of ICA and the effective disintegration of the pellicle was photographed.

Motility assay
Motility assays were performed as demonstrated by Whitaker et al. (2014) with little modifications. The assays were conducted on mLB agar with the absence (control) and presence of ICA (at its BIC) (treated). For swarming assay, a single colony of *V. parahaemolyticus* was picked using a sterile pipette tip and used to inoculate the surface of 1.5% mLB agar. The plates were incubated at 30 ℃ for 60 h and eventually the images were photographed. Swimming assays were performed with a single picked colony of the inoculum stabbed into mLB containing 0.3% agar and subsequently the images were photographed after incubation at 30 ℃ for 24 h.

Real time PCR
Total RNA was extracted from ICA treated and untreated cultures of *V. parahaemolyticus* (in mLB broth) using Trizol reagent and measured with BioSpec-nano spectrophotometer (Shimadzu, Japan). High-Capacity cDNA Reverse transcription kit (Applied Biosystems) was employed to convert RNA into cDNA. Quantitative real-time PCR was performed with Power SYBR® Green PCR master mix for a total of 10 µL reaction set up (ABI 7500, Applied Biosystems™). The thermal cycle was programmed for forty-cycle run under the following conditions; denaturation at 95 ℃ for 1 min; annealing at 58 ℃ for 30 s and extension at 72 ℃ for 40 s. Details of the primers used for this analysis are provided in Table 1. Samples were analyzed in triplicates and 16S rDNA gene was taken as the internal control for normalization. Gene expression was quantified by $2^{-\Delta\Delta CT}$ method (Salini & Pandian 2015).

Statistics
In the present study the entire experiments were carried out in triplicate. Data were expressed as arithmetic mean ± SD. Dunnett-ANOVA with statistical significance of $p < 0.05$ and $p < 0.01$ was used to compare the groups.

Results and discussion

Increased usage of antibiotics jeopardizes the therapeutic realm with antimicrobial resistance, which has made the proliferation of infectious diseases in an uncontrolled manner. *Vibrio parahaemolyticus*, a representative candidate of this regard, adopts both planktonic and biofilm mode of growth in submerged, inert and animate surfaces for its existence (Kaneko & Colwell 1975); and the long-term survival ability of the pathogen largely depends on the biofilm formation. Raw seafoods upon collection are refrigerated or stored at the freezing mode until use. During these adverse temperatures, the exopolysaccharide encased matrix protects the cells from declining phase and endure stability for longer periods. On reaching the ambient temperatures (20–35 ℃), bacteria redeem their growth from 10^2 to 10^3 CFU/g within 2–3 h (Elexon et al. 2014). In addition, this communal structure indirectly facilitates the safe entry of the pathogen by acquiring adaptive changes (regulated by the alternative σ factor RpoN) to reach the acidic stomach, whereby it assists in toxin secretion and other virulence factors responsible for disease succession (Whitaker et al. 2014). Hence, preventing the biofilm formation could effectively limit the spread of vibriosis caused by *V. parahaemolyticus*.

Among the 66 bacterial isolates screened, CFCS of *Marinomonas* sp. showed antibiofilm activity (data not shown) against *V. parahaemolyticus*. Further, the CFCS was processed for extract preparation through bioassay-guided fractionation. Amongst, ethyl acetate extract retained the biofilm inhibitory activity and it was subjected to column chromatography employing solvents based on their polarity. The column purified fraction dichloromethane: chloroform (50:50) inhibited the biofilm of *V. parahaemolyticus* (data not shown) and it was subjected to GC-MS analysis.

GC-MS analysis of the above column fraction resulted in 32-compound hits, which were identified with NIST (11) and Wiley (8) libraries (Fig. 1 and Table 2). Amongst, three compounds ICA, SA and DPA with major peak area were procured commercially and tested for their biofilm inhibitory potential against *V. parahaemolyticus*. While the compound ICA effectively inhibited the biofilm formation of *V. parahaemolyticus* ATCC 17802 by 71% and 89% at 200 and 400 µg/mL, respectively, DPA and SA failed to show any marked inhibition on the biofilms (Fig. 2). Based on the previous reports, which demonstrated the role of indole and its derivatives as antagonistic and antibacterial agents (Minivielle et al. 2013; Melander et al. 2014), ICA was employed for further assays and evaluation *in vitro*. The biofilm inhibitory concentration of ICA was taken as 200 µg/mL since broth dilution assay revealed considerable reduction in the cell density at 400 µg/mL and

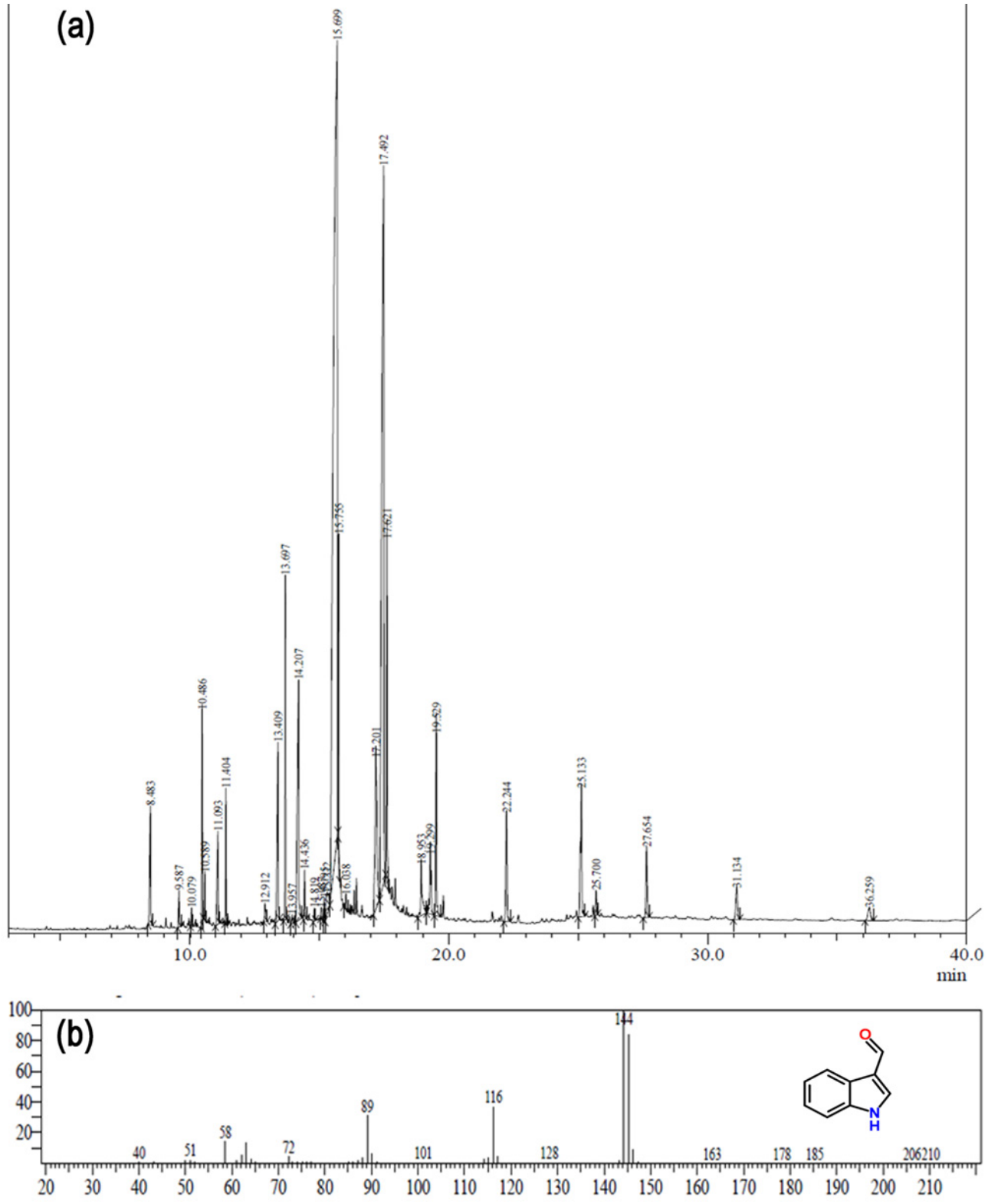

Fig. 1. (a) GC-MS analysis of the column-purified bioactive fraction chloroform: dichloromethane (50 : 50) of *Marinomonas* sp. (b) GC-MS spectra of the compound ICA in column-purified active fraction.

MIC was observed at 800 µg/mL. This visible inhibition of the cell growth was directly correlated with the spectrophotometric readings at OD_{600nm} (Fig. 3).

In addition, microscopic analysis also validated the inhibition of *V. parahaemolyticus* biofilms by ICA. Studies of LM and CLSM revealed marked reduction in the thickness of the biofilm as well as the microcolony formation compared to the control (Fig. 4). Remarkable differences were observed in parameters, such as biomass, maximum thickness and surface to volume ratio of the biofilm, which was substantiated using COMSTAT analysis (Table 3). SEM studies of the control

Table 2. List of compounds/hits identified from GC-MS analysis of column purified fraction of *Marinomonas* sp.

Peak	Retention time	Area	Area %	Name
1	8.483	21038959	1.53	Benzaldehyde, 4-hydroxy-
2	9.587	5260326	0.38	Ethanone, 1-(4-hydroxyphenyl)-
3	10.079	2305659	0.17	1H-Indol-4-ol
4	10.486	28403257	2.07	Phenol, 2,4-bis(1,1-dimethylethyl)-
5	10.589	4762077	0.35	Acetamide, N-(2-phenylethyl)-
6	11.093	17927286	1.31	Dodecanoic acid
7	11.404	13759969	1.00	1-Hexadecene
8	12.912	3894420	0.28	Ethanol, 2-(dodecyloxy)-
9	13.409	33566827	2.45	Tetradecanoic acid
10	13.697	35721667	2.60	1-Octadecene
11	13.957	1930764	0.14	Octadecanoic acid
12	14.207	63300592	4.61	1H-Indole-3-carboxaldehyde
13	14.436	6443875	0.47	Pentadecanoic acid
14	14.819	1671593	0.12	Ethanone, 1-(1H-indol-3-yl)-
15	15.087	1385645	0.10	Docosanoic acid, methyl ester
16	15.195	2386402	0.17	7,9-Di-tert-butyl-1-oxaspiro(4,5)deca-6,9-diene-2,8-dione
17	15.312	9553158	0.70	Cyclopentadecanone, 2-hydroxy-
18	15.699	550689864	40.13	l-(+)-Ascorbic acid 2,6-dihexadecanoate
19	15.755	32964455	2.40	n-Tetracosanol-1
20	16.038	2409340	0.18	Hexadecanoic acid
21	17.201	54230698	3.95	Cyclopentadecanone, 2-hydroxy-
22	17.492	276765482	20.17	Octadecanoic acid
23	17.621	44372882	3.23	1-Heptacosanol
24	18.953	15110942	1.10	Ricinoleic acid
25	19.299	18596682	1.36	(1,1'-biphenyl)-2,2'-diol, 3,3',5,5'-tetrakis(1,1-dim
26	19.529	31843622	2.32	1-Heptacosanol
27	22.244	24358534	1.78	1-Heptacosanol
28	25.133	32257673	2.35	1-Heptacosanol
29	25.700	4338973	0.32	2-[3-(trifluoromethyl)phenyl]-2,3-dihydro-1
30	27.654	14651504	1.07	Eicosyl heptafluorobutyrate
31	31.134	10225383	0.75	Eicosyl heptafluorobutyrate
32	36.259	6077152	0.44	Hexacosyl heptafluorobutyrate
		1372205662	100.00	

micrograph revealed a robust matrix of biofilm case largely coated with copious amount of extracellular matrix, within which the cells are embedded in piles. On the other hand, a single dispersed monolayer of biofilm was observed in ICA-treated micrograph with massive reduction in the extracellular polymeric substance. This clearly demonstrates the differences in the biofilm scaffold of ICA-treated and control samples.

Pellicle is a form of robust biofilms that occurs like dense mat of cohesive cells at the air-liquid interface, which defines the biofilm integrity, thickness and adhesion efficiency of the *Vibrio* spp. (Watnick & Kolter 1999; Enos-Berlage et al. 2005; Fong et al. 2006; Hollenbeck et al. 2014). In *V. parahaemolyticus*, complete formation of the pellicle was observed at 24 h of static culture incubated in the glass test tubes. With respect to the addition of ICA (300 µg/mL), complete disintegration of the pellicle was observed within 1 min (Fig. 5). This reveals the impact of ICA on the hydrophobic nature of the pathogen, since pellicle is strictly controlled by the transcription of *Vibrio* polysaccharide, an essential factor of extracellular matrix necessary for biofilm formation.

For environmental survival and human host colonization, *V. parahaemolyticus* utilizes two types of flagella. Single sheathed polar flagellum for its swimming motility in liquid culture and peritrichous lateral flag-

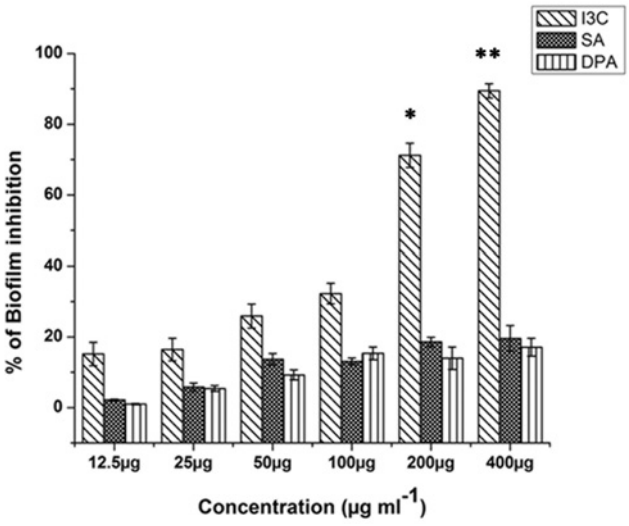

Fig. 2. Effect of compounds indole-3-carboxaldehyde (I3C), stearic acid (SA) and 2,6-di-O-palmitoyl-L-ascorbic acid (DPA) on *V. parahaemolyticus* biofilms. The assay was carried out in test tubes employing different concentrations of the compounds in marine LB broth with 1% inoculum. After 24 h of static incubation, the adhered biofilms were stained with 0.4% crystal violet, washed and quantified spectrophotometrically at OD_{570nm}. The experiments were carried out in triplicate and mean values with standard deviations are shown. The single and double asterisks indicate statistical significance $p < 0.05$ and $p < 0.01$, respectively, compared to control. Significant biofilm inhibition was observed with gradual increase in the concentration of ICA.

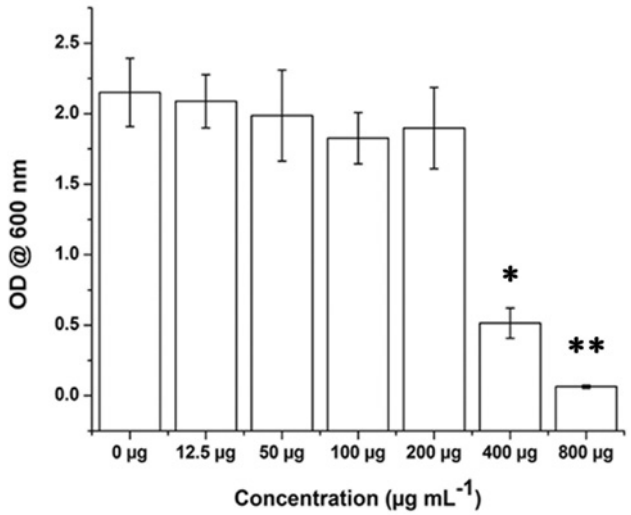

Fig. 3. Effect of ICA on the growth of *V. parahaemolyticus* at varying concentrations. Representative graph depicting the viability of control and ICA-treated planktonic cells at OD_{600nm} after 12 h of static incubation with 1% inoculum. The single and double asterisks indicate statistical significance $p < 0.05$ and $p < 0.01$, respectively, compared to control. A significant difference was found in the growth of ICA-treated planktonic cells at 400 and 800 µg/mL, respectively.

Table 3. COMSTAT analysis of the ICA treated and untreated (control) biofilms of *V. parahaemolyticus*.

Parameters	Control	Treated (200 µg/mL)
Biomass ($\mu m^3/\mu m^2$)	97.51625	21.93
Average thickness (µm)	91.78	20.64
Maximum thickness (µm)	91.78	20.64
Surface to volume ratio ($\mu m^2/\mu m^3$)	0.01496	0.05030

ella for swarming motility to move over surfaces. The pathogen converts its flagellar production from polar to lateral in response to surface sensing of the solid substrates, or growth under iron-limiting conditions. The swarming motility and biofilm forming ability are often related with the pathogenic potential of the bacteria (Kirov 2003). With reference to the QS mechanism in *V. parahaemolyticus*, it has been understood that biofilm formation, capsule production and swarming motility are directly controlled by the QS master regulator *opaR*. OpaR is the regulatory product of *opaR* gene in the QS system, which shares homology with LuxR protein of *Vibrio harveyi*. OpaR is responsible for controlling opacity to translucent colony type of the pathogen. OpaR regulates the capsular polysaccharide synthetic genes of *cps* locus in addition with lateral flagellar genes of *laf* system (McCarter 1998). The opacity of the pathogen depends on the capsular polysaccharides synthesis that, in turn, results in decreased biofilm formation and adherence to surfaces. At low cell density, with minimal amount of auto inducers, the cells acquire translucent morphology, which lacks capsule, and readily possess lateral flagella for swarming efficiency. On accumulation of auto inducers, at high cell density, QS cascade gets activated resulting in the activation of OpaR, which switches the cells from translucent to opaque form by hampering the production of lateral flagellar (*lafA*) genes (necessary for biofilm formation) and induces the CpsA synthesis (necessary for capsule production). In addition to *opaR*, *swrABC* signaling cascade is also present in *V. parahaemolyticus*, which involves GGDEF-EAL motif-containing sensory protein. Even though, it controls *cpsA* and *lafA* genes via modulating c-di-GMP levels, *opaR* regulation are utmost necessary for adaptive reversible phase variation (opaque-translucent). This phase variation is essential for the survival of the organism at varying surfaces, attachment and detachment, to develop in biofilms and to form structured communities (Boles & McCarter 2002; Broberg et al. 2011). Hence, quantifying the expression of these three genes *opaR, cpsA and lafA* could possibly reveal the mode of action of any biofilm inhibiting therapeutic molecule against this pathogen.

In order to evaluate the ability of ICA in modulating the QS pathway, motility assays and quantitative PCR were performed. In swarming motility assay, no movement was observed beyond the initial inoculum site on ICA-treated swarm agar compared to the control. Whereas, growth of the colony expanded in a regular fashion in the ICA-treated swim agar and no such enhanced expanded growth was observed in the control (Fig. 6). Additionally, the results of the quantitative PCR demonstrated the effect of ICA on the expression pattern of QS-mediated virulence genes and a $2^{-\Delta\Delta CT}$ method was employed to quantify the expression level (Fig. 7). Significant up-regulation was observed for *opaR* ($\sim$ 3 fold) and *cpsA* ($\sim$ 1.5 fold) and down-regulation was observed for *lafA* ($\sim$ 1.7 fold). Taken together, results of these assays evidenced the efficiency of ICA in activating OpaR, the master regulator, which as a consequence promoted the capsule (CpsA) production and retarded the swarming motility by repressing the lateral flagellar (LafA) production, which subsequently controlled the biofilm forming ability of the pathogen.

Indole and its derivatives are ubiquitous and are produced by more than 85 species of bacteria. Indole and most of its derivatives were known for their antibacterial, antifungal and antibiofilm properties (Lee & Lee 2010; Mansson et al. 2011). Interestingly, the indole producing and non-producing species were demonstrated to exhibit behavioral modification in response to exogenous indole. For example, *Vibrio cholerae* is known to be an indole producer, but some non-toxigenic strains of *V. cholerae* – *V. cholerae* SIO [isolated from seawater collected off the Scripps Institution of Oceanography (SIO)] and *V. cholerae* TP [obtained from plankton collected in the Torrey Pines Beach State Preserve estuary (TP)] restored the biofilm forming ability when provided with exogenous indole (Purdy et al. 2005; Mueller et al. 2009). On the other hand, the exogenous indole supplement reduced the biofilm forma-

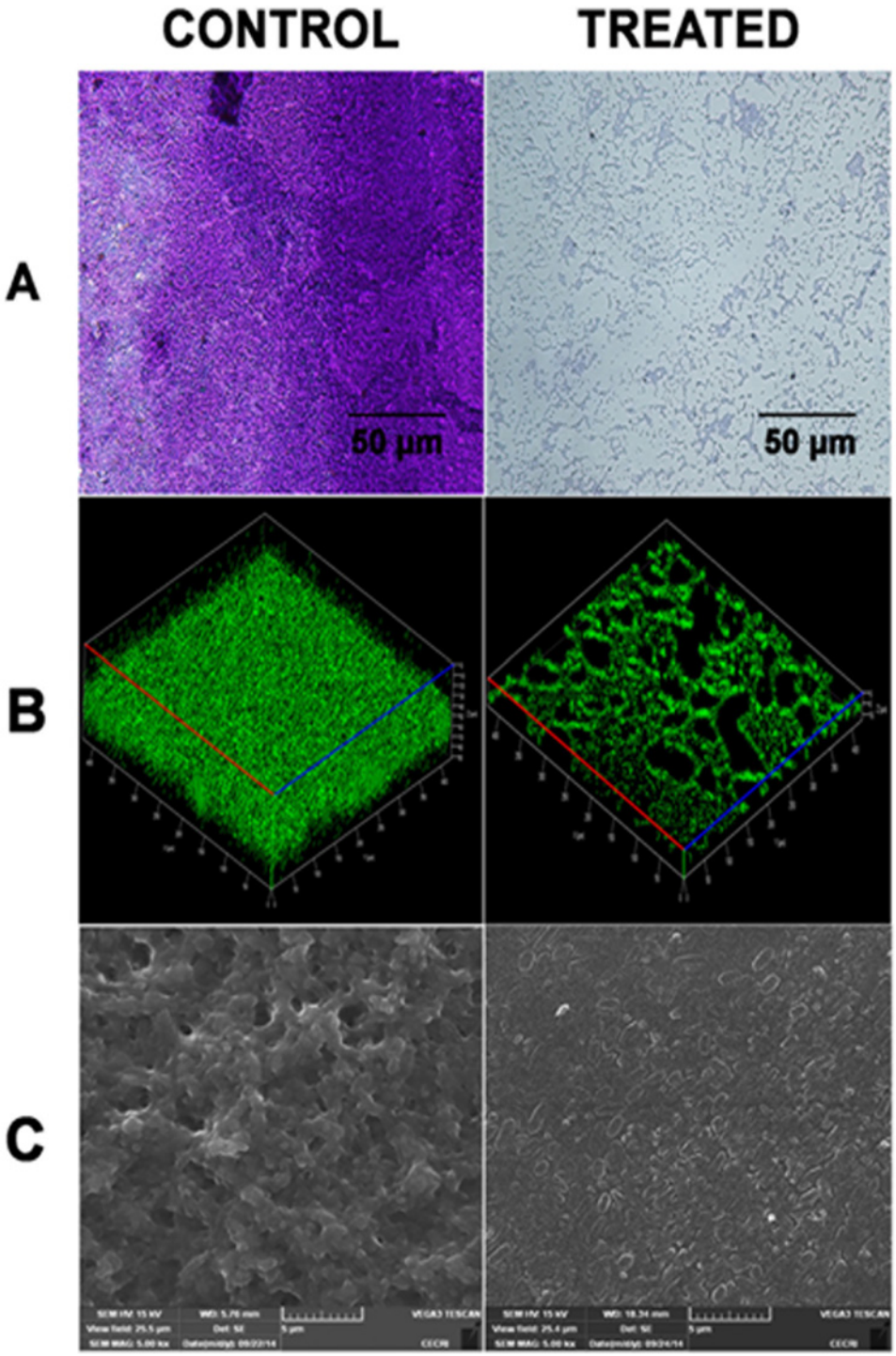

Fig. 4. Microscopic analysis of *V. parahaemolyticus* biofilm in the absence and presence of ICA at 200 µg/mL concentration. (A) Light microscopic images of biofilm (at 400× magnification) stained with crystal violet. (B) CLSM images of biofilm (at 200× magnification) stained with acridine orange. (C) SEM images of biofilm (at 5,000× magnification) are shown. The micrographs from light microscopy and CLSM clearly depict the antibiofilm activity of ICA. In addition, SEM micrograph with the scale 5 µm depicts the differences in the biofilm architecture of ICA-treated cells when compared to the control.

tion and motility of the clinically relevant *Escherichia coli* O157:H7. Derivatives of the indole were found to be more potent than indole as such in exhibiting antibiofilm activity. When indole decreased the biofilm formation of enterohemorrhagic *E. coli* O157:H7 by 6-fold, 7-hydroxy-indole decreased the biofilm formation by 10-fold (Lee et al. 2007; Rabin et al. 2015). Concerning the prevalence and distribution of indole from marine origin, some of its derivatives were synthesized by *Vibrio* species itself. Notably, Turbomycin and Vibrindole A produced by *V. parahaemolyticus* were found to exhibit profound antifungal activity (Bell et al. 1994; Veluri et al. 2003). Regarding the occurrence of ICA in natural sources, Lee et al. (2011) reported its discov-

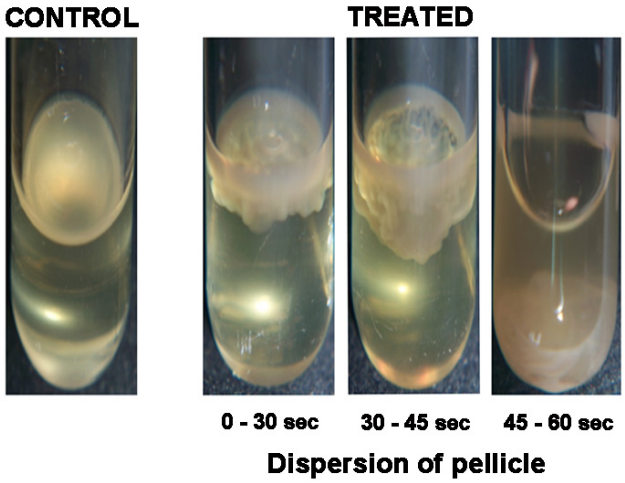

Fig. 5. Effect of ICA on *V. parahaemolyticus* pellicle. Photographs were taken during specific time intervals to indicate the complete removal of pellicle from adhered glass surface.

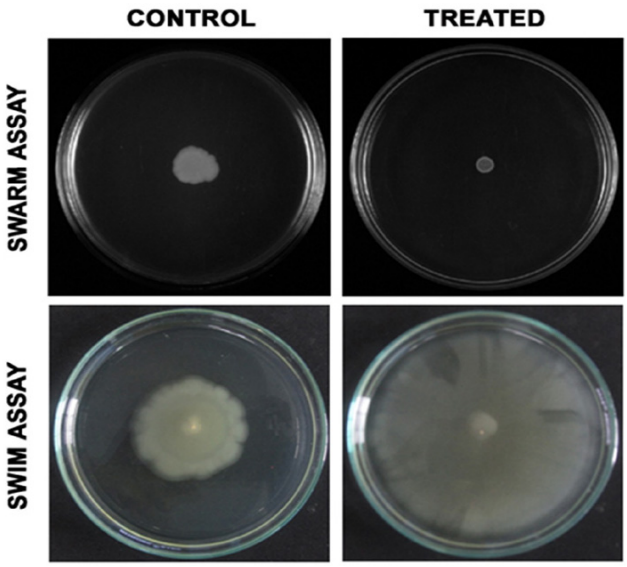

Fig. 6. Examination of *V. parahaemolyticus* motility in the absence and presence of ICA (200 μg/mL concentration).

ery from plant origin, which profoundly decreased the biofilm formation of *E. coli* O157:H7 and *Pseudomonas aeruginosa* by 11-fold and 1.9-fold, respectively, than indole as such. However, this is the first report deciphering the potential of ICA from marine bacterial origin exhibiting antibiofilm activity against *V. parahaemolyticus* ATCC 17802 *in vitro*.

Conclusion

In summary, the physiological and real-time gene expression assays accentuated the significant biofilm inhibiting ability of ICA by modulating the QS cascade of the pathogen, increasing the capsular polysaccharide synthesis and repressing lateral flagellar production. Further, investigation on the *in vivo* evaluation of ICA is expected to result in a good anti-adherent lead

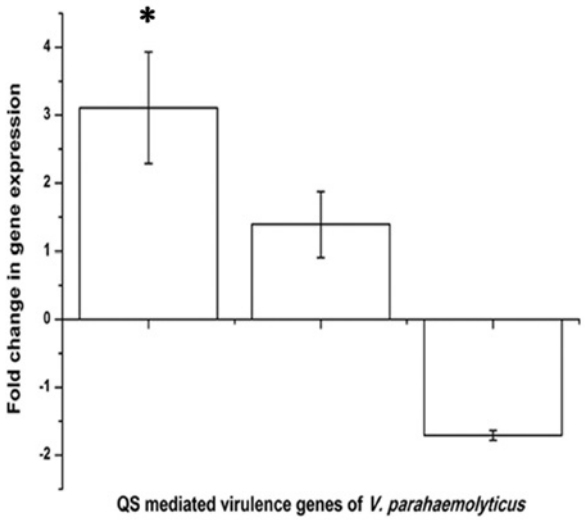

Fig. 7. Gene expression profiles of QS mediated virulence genes of *V. parahaemolyticus* in the presence of ICA at 200 μg/mL. Data are represented as mean ± standard deviation. The asterisk denotes the statistical significance of $p < 0.05$.

with potential for application in aquaculture industry as well as in clinical arena to treat *V. parahaemolyticus* biofilms.

Acknowledgements

The authors thankfully acknowledge the Bioinformatics Infrastructure Facility funded by Department of Biotechnology, Government of India [Grant No. BT/BI/25/012/2012 (BIF)], the instrumentation facility provided by Department of Science and Technology, Government of India through PURSE [Grant No.SR/S9Z-23/2010/42 (G)] & FIST (Grant No.SR-FST/LSI-087/2008), and University Grants Commission, New Delhi, through SAP-DRS1 [Grant No.F.3-28/2011 (SAP-II)].

References

Armstrong E., Boyd K.G. & Burgess J.G. 2000. Prevention of marine biofouling using natural compounds from marine organisms. Biotechnol. Annu. Rev. **6:** 221–241.

Bell R., Carmeli S. & Sar N. 1994. Vibrindole A, a metabolite of the marine bacterium *Vibrio parahaemolyticus*, isolated from the toxic mucus of the boxfish *Ostracion cubicus*. J. Nat. Prod. **57:** 1587–1590.

Boles B.R. & McCarter L.L. 2002. *Vibrio parahaemolyticus* scrABC, a novel operon affecting swarming and capsular polysaccharide regulation. J. Bacteriol. **184:** 5946–5954.

Broberg C.A., Calder T.J. & Orth K. 2011. *Vibrio parahaemolyticus* cell biology and pathogenicity determinants. Microbes Infect. **13:** 992–1001.

Ceccarelli D., Hasan N.A., Huq A. & Colwell R.R. 2013. Distribution and dynamics of epidemic and pandemic *Vibrio parahaemolyticus* virulence factors. Front. Cell Infect. Microbiol. **3:** 97–105.

Chowdhury G., Ghosh S., Pazhani G.P., Paul B.K., Maji D., Mukhopadhyay A.K. & Ramamurthy T. 2013. Isolation and characterization of pandemic and non pandemic strains of *Vibrio parahaemolyticus* from an outbreak of diarrhea in North 24 Parganas, West Bengal, India. Foodborne Pathog. Dis. **10:** 338–342.

Elexon N., Yay R., Nor A.M., Kantilal H.K., Ubong A., Yoshitsugu N., Nishibuchi M. & Son R. 2014. Biofilm assessment of

Vibrio parahaemolyticus from seafood using random amplified polymorphism DNA-PCR. Int. Food Res. J. **21:** 59–65.

Enos-Berlage J.L., Guvener Z.T., Keenan C.E. & Mc Carter L.L. 2005. Genetic determinants of biofilm development of opaque and translucent *Vibrio parahaemolyticus*. Mol. Microbiol. **55:** 1160–1182.

Fong J.C., Karplus K., Schoolnik G.K. & Yildiz F.H. 2006. Identification and characterization of RbmA, a novel protein required for the development of rugose colony morphology and biofilm structure in *Vibrio cholerae*. J. Bacteriol. **188:** 1049–1059.

Gowrishankar S., Poornima B. & Pandian S.K. 2014. Inhibitory efficacy of cyclo (L-leucyl-L-prolyl) from mangrove rhizosphere bacterium *Bacillus amyloliquefaciens* (MMS-50) towards cariogenic properties of *Streptococcus mutans*. Res. Microbiol. **165:** 278–289.

Hollenbeck E.C., Fong J.C., Lim J.Y., Yildiz F.H., Fuller G.G. & Cegelski L. 2014. Molecular determinants of mechanical properties of *Vibrio cholerae* biofilms at the air-liquid interface. Biophys. J. **107:** 2245–2252.

Kirov S.M. 2003. Bacteria that express lateral flagella enable dissection of the multifunctional roles of flagella in pathogenesis. FEMS Microbiol. Lett. **224:** 151–159

Kaneko T. & Colwell R.R. 1975. Adsorption of *Vibrio parahaemolyticus* onto chitin and copepods. Appl. Microbiol. **29:** 269–274.

Lee J., Bansal T., Jayaraman A., Bentley W.E. & Wood T.K. 2007. Enterohemorrhagic *Escherichia coli* biofilms are inhibited by 7-hydroxyindole and stimulated by isatin. Appl. Environ. Microbiol. **73:** 4100–4109.

Lee J.H., Cho M.H. & Lee J. 2011. 3-Indolylacetonitrile decreases *Escherichia coli* O157:H7 biofilm formation and *Pseudomonas aeruginosa* virulence. Environ. Microbiol. **13:** 62–73.

Lee J.H. & Lee J. 2010. Indole as an intercellular signal in microbial communities. FEMS Microbiol. Rev. **34:** 426–444.

Mansson M., Gram L. & Larsen T.Q. 2011. Production of bioactive secondary metabolites by marine Vibrionaceae. Mar. Drugs **9:** 1440–1468.

McCarter LL. 1998. OpaR, a homolog of *Vibrio harveyi* LuxR, controls opacity of *Vibrio parahaemolyticus*. J. Bacteriol. **180:** 3166–3173.

Melander R.J., Minivielle M.J. & Melander C. 2014. Controlling bacterial behavior with indole-containing natural products and derivatives. Tetrahedron **70:** 6363–6372.

Minivielle M.J., Bunders C.A. & Melander C. 2013. Indole/triazole conjugates are selective inhibitors and inducers of bacterial biofilms. Medchemcomm. **4:** 916–919.

Mueller R.S., Beyhan S., Saini S.G., Yildiz F.H. & Bartlett D.H. 2009. Indole acts as an extracellular cue regulating gene expression in *Vibrio cholerae*. J. Bacteriol. **191:** 3504–3516.

Nithya C., Devi M.G. & Pandian S.K. 2011. A novel compound from the marine bacterium *Bacillus pumilus* S6-15 inhibits biofilm formation in Gram-positive and Gram-negative species. Biofouling **27:** 519–528.

Newton A., Kendall M., Vugia D.J., Henao O.L. & Mahon B.E. 2012. Increasing rates of vibriosis in the United States, 1996-2010: review of surveillance data from 2 systems. Clin. Infect. Dis. **54:** 391–395.

Purdy A., Rohwer F., Edwards R., Azam F. & Barlett D.H. 2005. A glimpse into the expanded genome content of *Vibrio cholerae* through identification of genes present in environmental strains. J. Bacteriol. **187:** 2992–3001.

Qian P.Y., Li Z., Xu Y., Li Y. & Fusetani N. 2015. Mini-review: marine natural products and their synthetic analogs as antifouling compounds: 2009-2014. Biofouling **31:** 101–122.

Rabin N., Zheng Y., Opoku-Temeng C., Du Y., Bonsu E. & Sintim H.Q. 2015. Agents that inhibit bacterial biofilm formation. Future Med. Chem. **7:** 647–671.

Sahilah A.M., Laila R.A., Sallehuddin H.M., Osman H., Aminah A. & Ahmad Azuhairi A. 2014. Antibiotic resistance and molecular typing among cockle (*Anadara granosa*) strains of *Vibrio parahaemolyticus* by polymerase chain reaction (PCR)-based analysis. World J. Microbiol. Biotechnol. **30:** 649–659.

Salini R. & Pandian S.K. 2015. Interference of quorum sensing in urinary pathogen *Serratia marcescens* by *Anethum graveolens*. Pathog. Dis. **73:** ftv038.

Salini R., Sindhulakshmi M., Poongothai T. & Pandian S.K. 2015. Inhibition of quorum sensing mediated biofilm development and virulence in uropathogens by *Hyptis suaveolens*. Antonie van Leeuwenhoek **107:** 1095–1106.

Sayem S.M., Manzo E., Ciavatta L., Tramice A., Cordone A., Zanfardino A., De Felice M. & Varcamonti M. 2011. Anti-biofilm activity of an exopolysaccharide from a sponge-associated strain of *Bacillus licheniformis*. Microb. Cell. Fact. **10:** 74–85.

Shaw K.S., Rosenberg Goldstein R.E., He X., Jacibs J.M., Crump B.C. & Sapkota A.R. 2014. Antimicrobial susceptibility of *Vibrio vulnificus* and *Vibrio parahaemolyticus* recovered from recreational and commercial areas of Chesapeake Bay and Maryland Coastal Bays. PLoS One **9:** e89616.

Su Y.C. & Liu C. 2007. *Vibrio parahaemolyticus*: a concern of seafood safety. Food Microbiol. **24:** 549–558.

Veluri R., Oka I., Wagner-Dobler & Laatsch H. 2003. New indole alkaloids from the North sea bacterium *Vibrio parahaemolyticus* Bio249. J. Nat. Prod. **66:** 1520–1523.

Watnick P.I. & Kolter R. 1999. Steps in the development of a *Vibrio cholerae* biofilm. Mol. Microbiol. **34:** 586–595.

Whitaker W.B., Richards G.P. & Boyd E.F. 2014. Loss of sigma factor RpoN increases intestinal colonization of *Vibrio parahaemolyticus* in an adult mouse model. Infect. Immun. **82:** 544–556.

Yeung P.S. & Boor K.J. 2004. Epidemiology pathogenesis and prevention of food borne *Vibrio parahaemolyticus* infections. Foodborne Pathog. Dis. **1:** 74–88.

Received December 19, 2015
Accepted March 18, 2016